

Supporting Information

Immobilization of Brønsted Basic Hexaniobate on the Lewis Acidic Zirconia by an Emulsion Assisted Self-assembly Strategy for Synergistic Boosting Nerve Agent Simulant Decontamination

Huifang Liu,^a Xiangrong Sun,^c Jing Dong,^{b*} Chengpeng Liu,^a Wei Lu,^a Zhemi Xu,^b Ni Zhen,^a Di Zhang,^a Yingnan Chi,^{a*} Changwen Hu^a

^aKey Laboratory of Cluster Science Ministry of Education, Beijing Key Laboratory of Photoelectroic/Electrophotonic Conversion Materials, School of Chemistry and Chemical Engineering, Beijing Institute of Technology, Beijing, 100081, People's Republic of China.

^bCollege of Chemistry and Materials Engineering, Beijing Technology and Business University, 11 Fucheng Road, Beijing, 100048, People's Republic of China.

^cJiaxiang Country Branch of Jining Municipal Ecology and Environment Bureau, Jining, 272400, People's Republic of China.

Table of Contents

1. Experimental section

1.1 Preparation of amphiphilic $[C_{16}H_{33}N(CH_3)_3]_4K_3HNb_6O_{19}$

1.2 Preparation of ZrO_2

2. Characterization of the as-prepared catalysts

Figure S1. The confocal microscopy images of the emulsion formed with $C_{16}N-Nb_6$

Figure S2. The FT-IR spectra of the as-prepared catalyst

Figure S3. Thermogravimetric curves of $C_{16}N-Nb_6/ZrO_2$ and $C_{16}N-Nb_6$

Figure S4. The survey XPS spectrum of $C_{16}N-Nb_6/ZrO_2$ composite

Figure S5. XRD patterns of $C_{16}N-Nb_6/ZrO_2$, $C_{16}N-Nb_6$ and ZrO_2

Figure S6. Images of water contact angles of $C_{16}N-Nb_6/ZrO_2$, $C_{16}N-Nb_6$ and ZrO_2

Table S1. The elemental analysis of the as-prepared catalysts

Table S2. The surface area and porosity data of $C_{16}N-Nb_6/ZrO_2$ and ZrO_2 .

3. Catalytic decontamination of DMNP and CEES

Figure S7. ^{31}P NMR of DMNP hydrolysis over different catalysts

Figure S8. ^{31}P NMR of DMNP hydrolysis over ZrO_2 at pH = 9.3

Figure S9. FT-IR spectra of $C_{16}N-Nb_6/ZrO_2$ before and after the catalytic hydrolysis reaction

Figure S10. Mass spectrum of CEESO

Figure S11. Mass spectrum of $CEESO_2$

Figure S12. Raman spectra of ZrO_2 before and after treating with aqueous H_2O_2

Figure S13. FT-IR spectra of $C_{16}N-Nb_6/ZrO_2$ before and after the oxidative decontamination reaction

Table S3. Comparison of the different catalysts for the hydrolytic activity.

4. References

1. Experimental Section

All the starting chemicals and solvents were reagent grade, purchased from commercial sources and used without further purification. $\text{K}_7\text{HfNb}_6\text{O}_{19} \cdot 13\text{H}_2\text{O}$ was synthesized according to the reported method^[1].

1.1 Preparation of amphiphilic $[\text{C}_{16}\text{H}_{33}\text{N}(\text{CH}_3)_3]_4\text{K}_3\text{HfNb}_6\text{O}_{19}$

$[\text{C}_{16}\text{H}_{33}\text{N}(\text{CH}_3)_3]_4\text{K}_3\text{HfNb}_6\text{O}_{19}$ ($\text{C}_{16}\text{N-Nb}_6$) was prepared according to the reported method^[2]. $[\text{C}_{16}\text{H}_{33}\text{N}(\text{CH}_3)_3]\text{Br}$ (1.0 g) was fully dissolved in deionized water (50 ml) under ultrasonic condition to obtain solution A. $\text{K}_7\text{HfNb}_6\text{O}_{19} \cdot 8\text{H}_2\text{O}$ (0.05 mmol) was dissolved in 80 mL NaH_2PO_4 - Na_2HPO_4 buffer solution (0.2 M, pH = 8.2) to obtain solution B. The solution B was injected into solution A and stirred rapidly for 1 h at room temperature. And then, the obtained white precipitate was collected by centrifugation and washed with deionized water for 3 times. Finally, the white precipitate was dried under oven at 60°C overnight to obtain amphiphilic $\text{C}_{16}\text{N-Nb}_6$.

1.2 Preparation of zirconia

Zirconium *n*-butoxide (0.5 mL) was dropped into deionized water (10 mL, ice-bath) with continuous stirring. After 30 min, the ZrO_2 product was obtained by filtration, washing and drying.

2. Characterization of the as-prepared catalysts

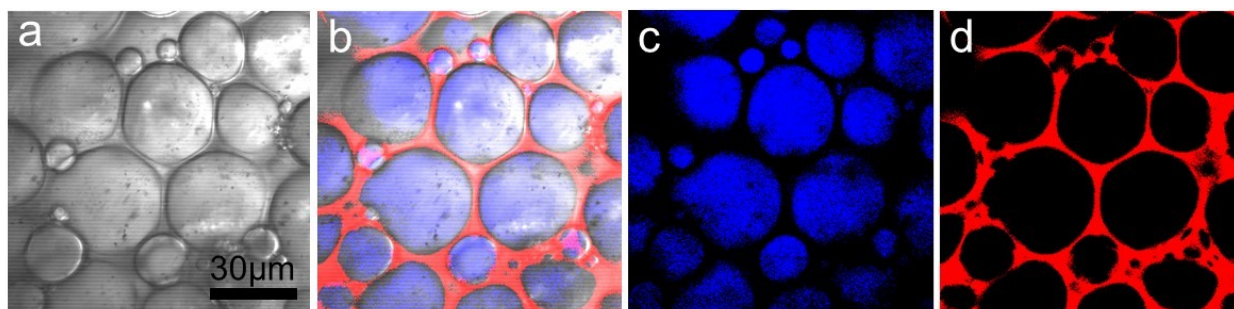


Figure S1. The confocal microscopy images of water-in-oil type emulsion formed with $C_{16}N-Nb_6$ in the mixture solution of water and toluene, where the oil phase was stained with Nile Red (red) and the water phase was stained with polydopamine quantum dots (blue). (a) Without laser irradiation. (b) Both the polydopamine quantum dots in water phase and the Nile Red in oil phase were simultaneously irradiated. (c) Only the polydopamine quantum dots in water phase were irradiated; (d) Only with the Nile Red in oil phase was irradiated.

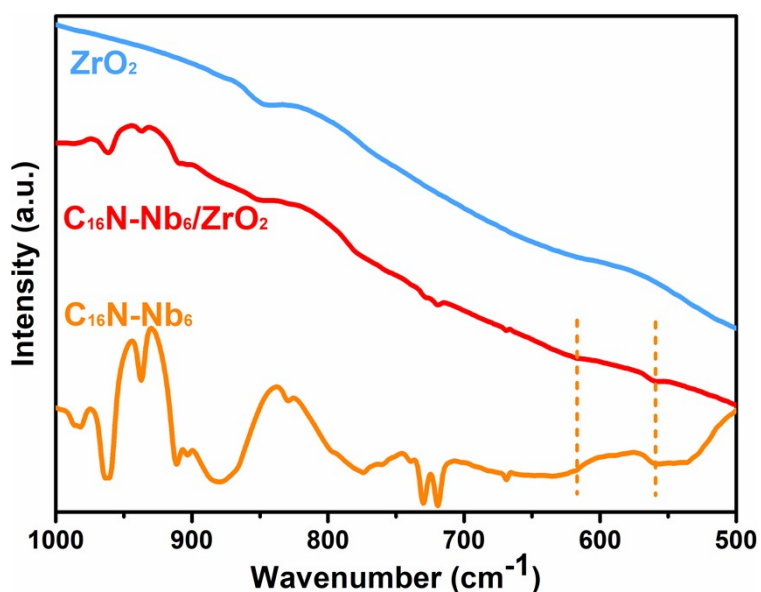


Figure S2. The FT-IR spectra of $C_{16}N-Nb_6/ZrO_2$, $C_{16}N-Nb_6$ and ZrO_2 in the region of 500-1000 cm^{-1} .

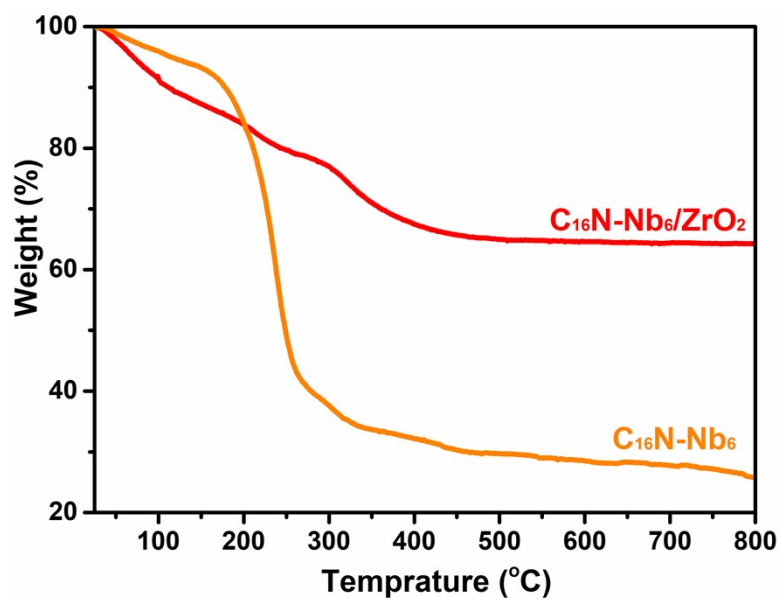


Figure S3. Thermogravimetric curves of 11%- $C_{16}N-Nb_6/ZrO_2$ and $C_{16}N-Nb_6$.

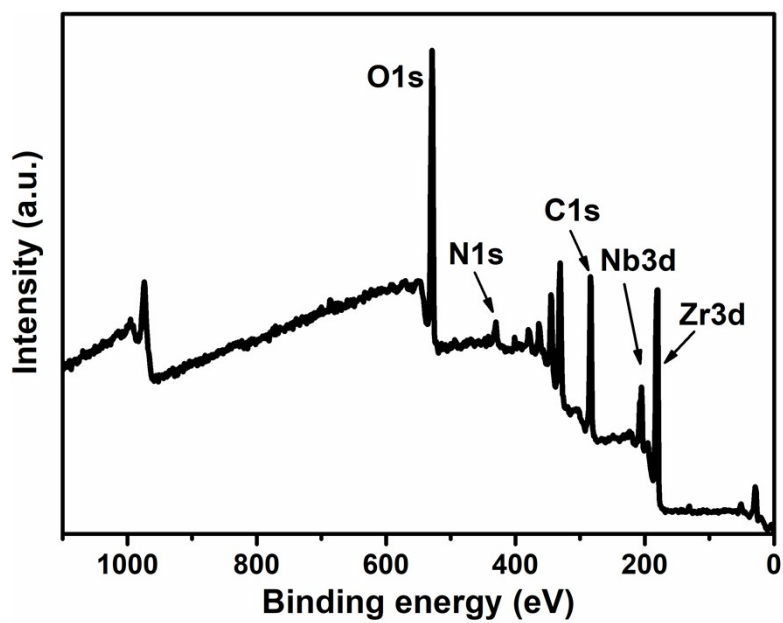


Figure S4. The survey XPS spectrum of the $C_{16}N-Nb_6/ZrO_2$ composite.

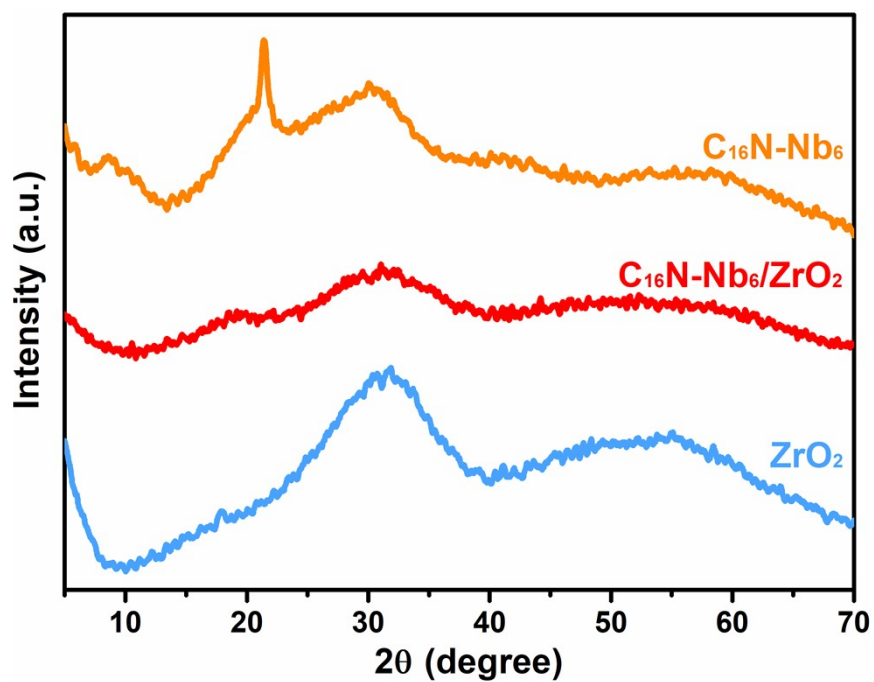


Figure S5. XRD patterns of $C_{16}N-Nb_6/ZrO_2$, $C_{16}N-Nb_6$ and ZrO_2 .



Figure S6. Images of water contact angles of $C_{16}N-Nb_6$, ZrO_2 and $C_{16}N-Nb_6/ZrO_2$.

3. Catalytic decontamination of DMNP and CEES

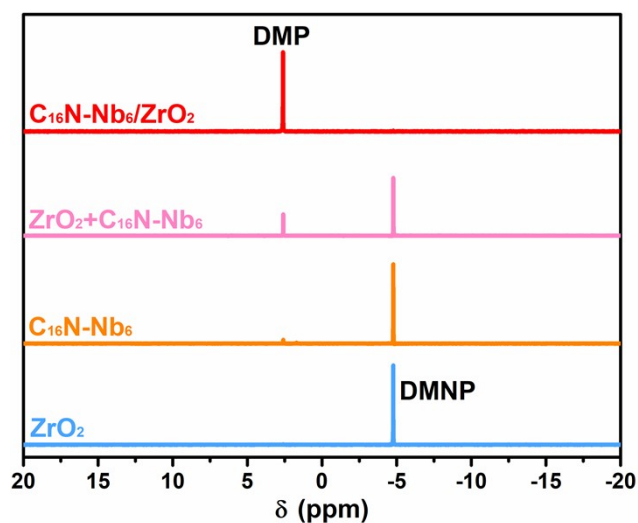


Figure S7. ^{31}P NMR of DMNP hydrolysis over different catalysts after 6 h. Reaction conditions: DMNP (5 mg), H_2O (300 μL), CD_3CN (200 μL), catalyst (1.7 mg for $\text{C}_{16}\text{N-Nb}_6$, 13.3 mg for ZrO_2), room temperature for 6 h.

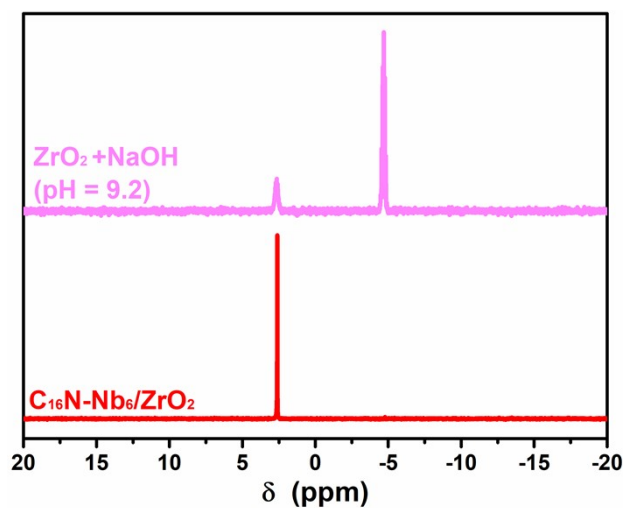


Figure S8. ^{31}P NMR of DMNP hydrolysis over ZrO_2 at pH = 9.3 after 6 h. Reaction conditions: DMNP (5 mg), H_2O (300 μL), CD_3CN (200 μL), ZrO_2 (13.3 mg), room temperature for 6 h.

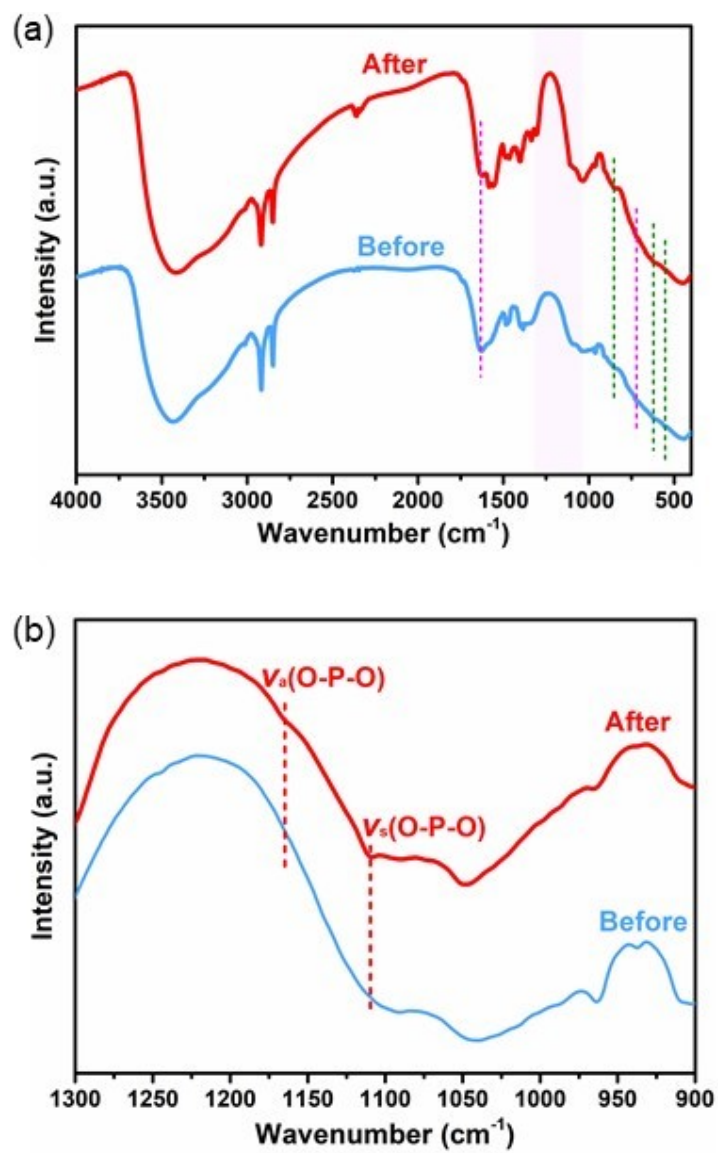


Figure S9. FT-IR spectra of $\text{C}_{16}\text{N-Nb}_6/\text{ZrO}_2$ before and after the catalytic hydrolysis reaction.

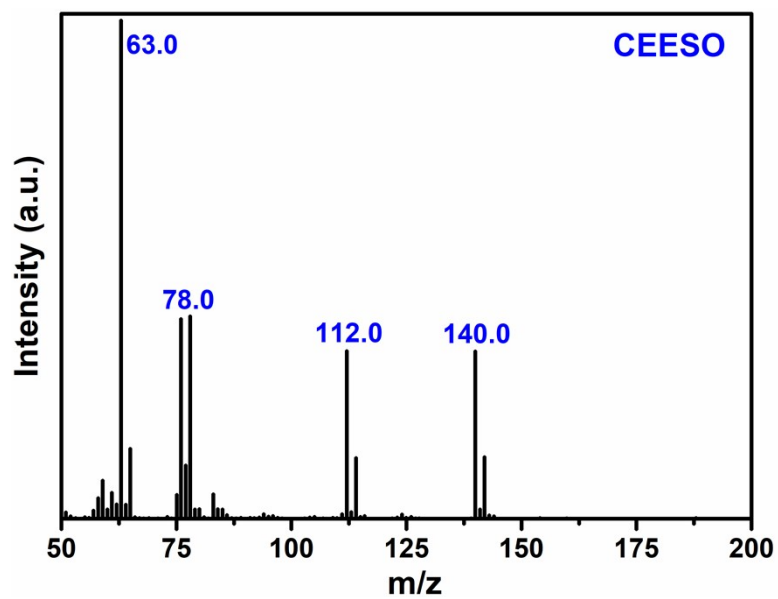


Figure S10. Mass spectrum of CEESO.

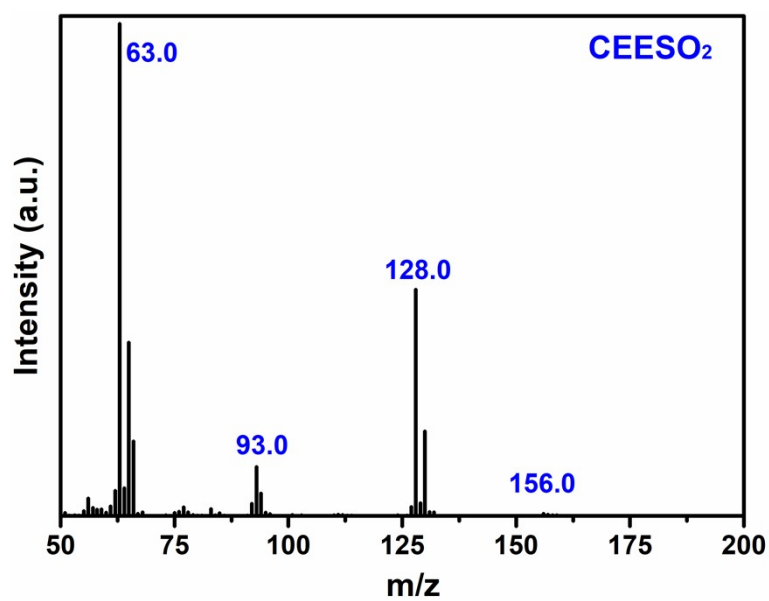


Figure S11. Mass spectrum of CEESO₂.

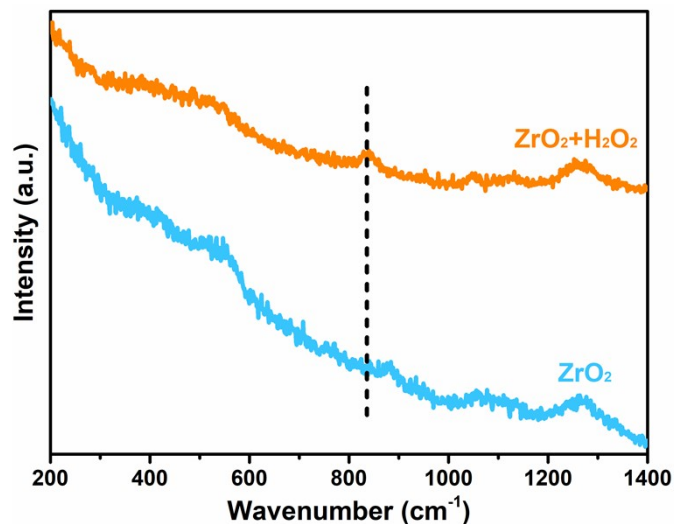


Figure S12. Raman spectra of ZrO₂ before (blue line) and after (orange line) treating with aqueous H₂O₂. A new peak at 838 cm⁻¹ was assigned to O-O stretching appeared after treating the ZrO₂ with H₂O₂, suggesting a Zr-peroxo species might be also responsible for the oxidative decontamination reaction.

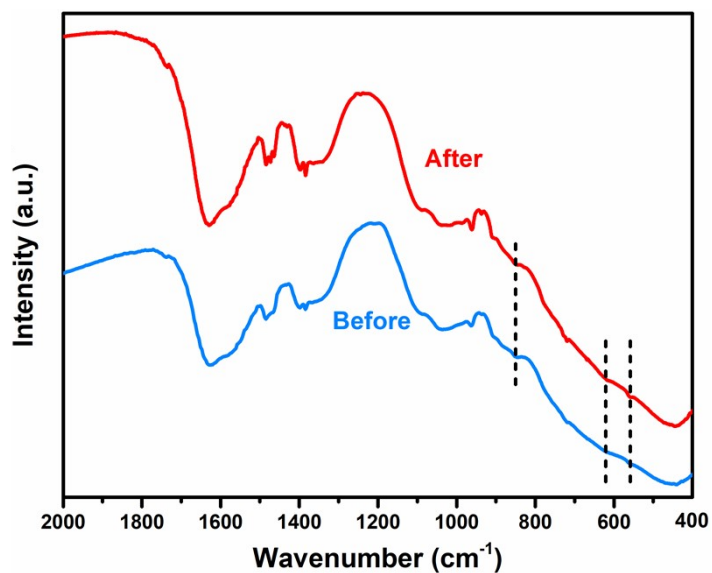


Figure S13. FT-IR spectra of C₁₆N-Nb₆/ZrO₂ before and after the oxidative decontamination reaction.

Table S1. The elemental analysis of the as-prepared C₁₆N-Nb₆/ZrO₂ catalysts.

Composite	Mass ratio of C ₁₆ N-Nb ₆ and ZrO ₂	Calculated loading amount of C ₁₆ N-Nb ₆ (wt%)
C ₁₆ N-Nb ₆ /ZrO ₂ -19%	3:5	19.3
C ₁₆ N-Nb ₆ /ZrO ₂ -11%	1:3	11.6
C ₁₆ N-Nb ₆ /ZrO ₂ -9%	1:4	9.1
C ₁₆ N-Nb ₆ /ZrO ₂ -6%	1:6	6.7
C ₁₆ N-Nb ₆ /ZrO ₂ -4%	1:8	4.5

Table S2. The surface area and porosity data of C₁₆N-Nb₆/ZrO₂ and ZrO₂.

Sample	S _{BET} (m ² /g)	Pore volume (cm ³ /g)	Average Pore Diameter (nm)
C ₁₆ -Nb ₆ /ZrO ₂	41.6	0.27	25.9
ZrO ₂	242.8	0.39	6.4

Table S3. Comparison of the different catalysts for the hydrolytic decontamination of nerve agent simulants under basic additive free conditions.

Entry	Catalyst	Simulant	Conv. (%)	Time	System	Ref.
1	C ₁₆ N-Nb ₆ /ZrO ₂	DMNP	100	6 h	heterogeneous	This work
2	MOF-808	POX ^[f]	0	35 min	heterogeneous	3
3	NU-1000	POX	0	35 min	heterogeneous	3
4	UiO-66-NH ₂	POX	~20	35 min	heterogeneous	3
5	{[PW ₁₁ Zr] ₂ } ^[a]	DMNP	100	120 h	homogeneous	4
6	{Sc ₂ PW ₁₀ } ^[b]	DMNP	97	9 h	homogeneous	5
7	{GeNb ₁₂ } ^[c]	DMMP ^[g]	54	264 h	heterogeneous	6
8	{Nb ₄₇ } ^[d]	DMMP	46	263 h	homogeneous	7
9	{Nb ₅₄ } ^[e]	DMMP	40	264 h	heterogeneous	8
10	Zr(OH) ₄ -fiber	DFP ^[h]	62	24 h	solid phase ^[i]	9

[a] {[PW₁₁Zr]₂}: (Et₂NH₂)₈{[α-PW₁₁O₃₉Zr(μ-OH)(H₂O)]₂}·7H₂O.

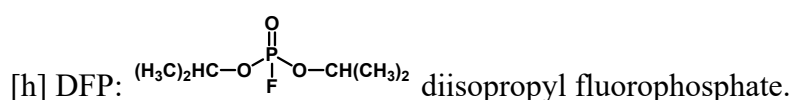
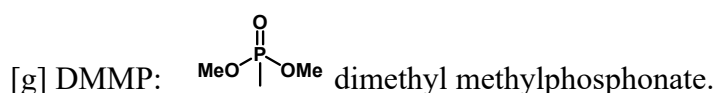
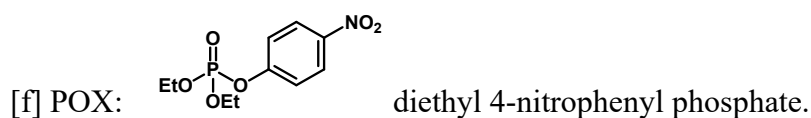
[b] {Sc₂PW₁₀}: Na₇[Sc₂(CH₃COO)₂PW₁₀O₃₈]·10H₂O·2CH₃COONa.

[c] {GeNb₁₂}: K₁₂[T₁₂O₂][GeNb₁₂O₄₀]·19H₂O.

[d] {Nb₄₇}: H₂Li₅Na₃K₅[Cu(en)₂]₇[Nb₄₇O₁₂₈(OH)₆(CO₃)₂]·20H₂O, en = ethylenediamine.

[e] {Nb₅₄}: H₅Na₇K₄[Cu(en)₂]₂[Cu(en)(H₂O)]₂[Cu(en)₂(H₂O)]₄[Nb₅₄O₁₅₁]·27H₂O,

en = ethylenediamine.



[i] Zr(OH)₄-fiber is soaked by DFP at room temperature with a proper humidity level.

4. References

- [1] C. M. Flynn Jr., G. D. Stucky, *Inorg. Chem.*, 1969, **8**, 332-334.
- [2] X. Q. Li, J. Dong, H. F. Liu, X. R. Sun, Y. N. Chi, C. W. Hu, *J. Hazard. Mater.*, 2018, **344**, 994-999.
- [3] M. C. Koning, M. v. Grol, T. Breijaert, *Inorg. Chem.*, 2017, **56**, 11804-11809.
- [4] D. L. Collins-Wildman, M. Kim, K. P. Sullivan, A. M. Plonka, A. I. Frenkel, D. G. Musaev, C. L. Hill, *ACS Catal.*, 2018, **8**, 7068-7076.
- [5] D. Zhang, W. Q. Zhang, Z. G. Lin, J. Dong, N. Zhen, Y. N. Chi, C. W. Hu, *Inorg. Chem.*, 2020, **59**, 9756-9764.
- [6] W. W. Guo, H. J. Lv, K. P. Sullivan, W. O. Gordon, A. Balboa, G. W. Wagner, D. G. Musaev, J. Bacsá, C. L. Hill, *Angew. Chem. Int. Ed.*, 2016, **55**, 7403-7407.
- [7] Y. L. Wu, X. X. Li, Y. J. Qi, H. Yu, L. Jin, S. T. Zheng, *Angew. Chem. Int. Ed.*, 2018, **57**, 8572-8576.
- [8] Y. L. Wu, Y. J. Wang, Y. Q. Sun, X. X. Li, S. T. Zheng, *Chem. Commun.*, 2011, **58**, 3322-3325.
- [9] S. Kim, W. B. Ying, H. Jung, S. G. Ryu, B. Lee, K. J. Lee, *Chem. Asian J.*, 2017, **12**, 698-705.